



Published in final edited form as:

*Nano Lett.* 2009 January ; 9(1): 485–490. doi:10.1021/nl803621x.

## Dimers of Silver Nanospheres: Facile Synthesis and Their Use as Hot Spots for Surface-Enhanced Raman Scattering

Weiyang Li, Pedro H. C. Camargo, Xianmao Lu, and Younan Xia\*

*Department of Biomedical Engineering, Washington University, Saint Louis, Missouri 63130*

### Abstract

This paper describes a simple, one-pot method that generates dimers of silver nanospheres in one step without any additional assembly steps. The dimers are consisted of single-crystal silver nanospheres ~30 nm in diameter and separated by a gap of 1.8 nm wide. The key to the success of this method lies in the control of colloidal stability and oxidative etching by optimizing the amount of chloride added to a polyol synthesis. The dimers provide a well-defined system for studying the hot spot phenomenon (hot spot: the gap region of a pair of strongly coupled silver or gold nanoparticles), an extremely important but poorly understood subject in surface-enhanced Raman scattering (SERS). Because of the relatively small size of the silver nanospheres, only those molecules trapped in the hot spot region are expected to contribute to the detected SERS signals. By correlating SERS measurements with SEM imaging, we found that the SERS enhancement factor within the hot spot region of such a dimer was on the order of  $2 \times 10^7$ .

There has been a rapidly growing interest in controlling the assembly of silver or gold nanoparticles into well-defined structures for surface-enhanced Raman scattering (SERS) applications.<sup>1-3</sup> The electromagnetic field in the gap region of a pair of strongly coupled nanoparticles can be drastically amplified, resulting in an extraordinary enhancement factor large enough for single-molecule detection.<sup>4-6</sup> In this so-called hot spot phenomenon, it is critical to achieve a precise control over the following parameters: the size, shape, and crystallinity of the nanoparticles, as well as the spacing between the nanoparticles. Although the hot spot phenomenon has been extensively investigated from both theoretical and experimental perspectives, it remains an elusive, feebly understood subject. Part of the reason can be attributed to the poor control involved in the preparation of hot spots via salt-induced colloidal agglomeration, a process that typically leads to the formation of aggregates of all different sizes together with a broad distribution in terms of interparticle spacing. The nanoparticles used in these studies were also troubled by nonuniformity in terms of size, shape, and crystallinity.

Some progress has been made in controlling the assembly of silver or gold nanoparticles into specific structures.<sup>7-10</sup> Most of these studies rely on the decoration of the nanoparticle surface with “binding patches” derived from synthetic organic or biological molecules.<sup>11-16</sup> For example, Alivisatos et al. and Mirkin et al. have pioneered the use of DNAs to assemble gold nanoparticles into dimers, trimers, and larger structures;<sup>11-14</sup> Feldheim et al. have prepared small clusters of gold nanoparticles via rigid, multivalent thiol-linkers;<sup>15</sup> Shumaker-Parry et al. have produced dimers of gold nanoparticles using organic molecules through an asymmetric functionalization pathway.<sup>16</sup> Recently, Chen et al. prepared polymer-encapsulated dimers of

\* To whom correspondence should be addressed. E-mail: xia@biomed.wustl.edu..

**Supporting Information Available:** A detailed description of the experimental procedures is provided. This material is available free of charge via the Internet at <http://pubs.acs.org>.

gold nanoparticle by functionalizing the surface of gold particles with a thiol-terminated hydrophobic ligand.<sup>17</sup> In general, the procedures for producing a dimeric structure through surface modification are rather complicated, usually involving a number of steps. On the other hand, the resultant dimers are limited in use for SERS applications because the biological or organic linkers that bridge the two nanoparticles tend to prevent the analyte molecules from entering the hot spot. It still remains a grand challenge in assembling silver or gold nanoparticles into dimers with well-defined hot spots for SERS.

Here we describe a simple and versatile method for generating dimers of single-crystal silver nanospheres with reasonably high yields in one step. We focused on silver because it has been shown to outperform gold by many folds in SERS detection.<sup>18</sup> Our synthesis is based upon the polyol process<sup>19</sup> in which ethylene glycol (EG) serves as a solvent and a precursor to the reducing agent. By introducing a small amount of sodium chloride into the reaction solution,<sup>20</sup> we could obtain single-crystal silver nanoparticles as a result of oxidative etching and at the same time induce dimerization due to a change to colloidal stability. In a typical synthesis, we obtained dimers consisting of silver nanospheres ~30 nm in diameter and separated by 1.8 nm in the solution phase with a yield >50%. Because of the relatively small size of the silver nanospheres, only those molecules trapped in the hot spot are expected to contribute to the detected SERS signals, making these dimers an ideal system for studying the hot spot phenomenon.

Figure 1A shows a typical TEM image of the product obtained at 20.5 h into the reaction with the addition of 90  $\mu$ L NaCl/EG solution into the mixture. Black circles were drawn to highlight the dimers. Counting over 150 silver nanoparticles, we found that ~58% of them had dimerized during the synthesis. To confirm that the dimers were formed in the reaction solution rather than during TEM sample preparation, we added tetraethylorthosilicate (TEOS) to the reaction mixture to fix the dimers via silica coating. In a typical process, the as-prepared sample was mixed with 1.5 mL of ethanol; 0.2 mL of this mixture was then transferred into a solution of 3 mL of ethanol and 0.5 mL of deionized water. Under continuous magnetic stirring, 65  $\mu$ L of 30% ammonia solution and 10  $\mu$ L of TEOS were sequentially added. After the reaction had proceeded for 4 h, the solution was centrifuged at 6000 rpm to isolate the precipitate, which was then redispersed in ethanol for further characterization. Figure 1B shows a TEM image of the silica-coated sample. Many dimers can be easily identified in this sample, clearly demonstrating the presence of dimers in the reaction solution. The inset in Figure 1B shows a magnified TEM image of the same sample. The clear contrast between the core and shell indicates that the silica coating had a uniform thickness of ~7 nm over the entire surface of the dimer.

Figure 1C shows a magnified TEM image of an individual dimer, implying a spherical shape for the two silver nanoparticles that were 30.0 and 31.7 nm in diameter. There is a narrow gap of 1.8 nm wide between the two nanospheres, forming the so-called hot spot region. On the basis of our previous studies,<sup>21</sup> the silver nanospheres obtained using this protocol were actually truncated octahedrons with a rounded profile (see the inset of Figure 1C), which are enclosed by a mix of {111} and {100} facets. The uniform contrast across each particle indicates that the silver nanospheres were single crystalline, which is also supported by HRTEM imaging. As shown in Figure 1D, each sphere displayed a periodic fringe with an interplanar spacing of 0.24 nm, a value that is consistent with the separation between the {111} lattice planes. As labeled in the same Figure, the top sphere interacted with the bottom sphere through one of its {111} facets. In a truncated octahedron, the angle between adjacent {111} facets is 73.2°, indicating that the facet used by the bottom sphere to interact with the top sphere was also {111}. All these results are supported by our previous observations, where PVP was found to interact more strongly with the {100} than {111} facets,<sup>22</sup> and thus preferentially adsorb on the {100} facets. When two silver nanospheres approached each other, it was not

unreasonable to expect that they would prefer to interact through the {111} rather than {100} facets.

To further understand and monitor the evolution of dimers, we took samples at various stages of the reaction as guided by the distinctive color changes. Within the first minute of reaction, the solution turned into light yellow, indicating the formation of silver nanoparticles due to polyol reduction. The yellow color kept increasing in intensity and maintained its appearance for another 20 min. Our previous experiments showed that most of the particles were twinned at this time.<sup>19</sup> As the reaction proceeded, the yellow color started to fade and became colorless after about 1 h due to the oxidative etching of twinned nanoparticles in the solution. The solution remained colorless for a long period of time until a light yellow color reappeared about 19 h into the synthesis (the time at which the reaction mixture became light yellow again was more or less different for different syntheses, so the state of the reaction should be told from the color change rather than a specific time). Figure 2A shows a TEM image of the sample when the reaction mixture turned into light yellow again after oxidative etching. The inset in Figure 2A gives a TEM image at a higher magnification. It is clear that the sample at this point contained many dimers, but the nanospheres in the dimers were very small with their diameters being in the range of 8–10 nm. When the reaction was continued, the color of the reaction mixture became darker. Figure 2B shows a TEM image of particles sampled 1.5 h later when the reaction mixture exhibited a bright yellow color with a slight orange tint. Compared to the sample shown in Figure 2A, the silver nanospheres increased to ~30 nm in diameter as shown by the magnified TEM image (inset of Figure 2B). As the reaction was continued for another 0.5 h, the solution became dark orange-yellow with a slight red-brown tint. From the TEM images (Figure 2C), we can see that the silver particles grew a little bigger and their shapes became more or less cubic, not as spherical as those shown in Figure 2B. In addition, we found that instead of approaching each other through the {111} facets as shown in Figure 1C, the silver nanoparticles with a cubic shape could also interact with each other through their {100} facets. This is because the particles had evolved into cubes with only slight truncation at corners and thus mainly enclosed by {100} facets due to the preferential stabilization of these facets by PVP.<sup>22</sup> This observation suggests that the two silver nanoparticles in the dimer could freely rotate in space during the synthesis, reflecting the dynamic aspect of the dimeric structure.

Figure 2D shows UV–vis spectra taken from samples at these three different reaction stages in correspondence to the products shown in Figure 2A–C, respectively. The inset in Figure 2D shows photographs of these samples dispersed in ethanol. Note that the localized surface plasmon resonance (LSPR) peak at 400 nm associated with the silver nanoparticles gradually increased in intensity as the reaction proceeded. It is worth noting that a shoulder peak appeared in the range of 450 to 550 nm for samples in Figure 2B,C, which could be attributed to dimerization. It is worth pointing out that spectrum B agrees well with the extinction spectrum calculated for dimers of silver nanospheres,<sup>23</sup> further confirming the formation of dimers in the reaction solution. Additionally, there was a slight red shift for the main peak as the reaction proceeded, which could be ascribed to the growth of particle size.

The yield of the dimers is sensitive to the concentration of NaCl in the reaction mixture. Figure 3A shows a TEM image of the sample when a smaller amount (66 rather than 90  $\mu\text{L}$ ) of NaCl/EG solution was added to the reaction. In this case, both single-crystal and multiply twinned nanoparticles were formed, but there was essentially no dimer in the sample. This observation can be explained by the oxidative etching scheme outlined in our previous studies.<sup>20</sup> According to this scheme, a combination of oxygen from air and a ligand for the metal ion (such as chloride for  $\text{Ag}^+$ ) in the reaction solution can result in a powerful etchant for both the nuclei and seeds. In the presence of sufficient chloride, the defects inherently present on twinned particles will provide more reactive sites for oxidative dissolution, while single-crystal seeds are more resistant to oxidative etching as there are no twin boundary defects on the surface. As clearly

shown in Figure 3A, both single-crystal and twinned particles were formed when not enough NaCl was added. In contrast, when a larger amount (114  $\mu\text{L}$ ) of the NaCl/EG solution was added to the reaction, dimers of single-crystal Ag nanospheres could also be produced, as shown in Figure 3B. However, it is clear that the yield of dimers was much lower than the sample shown in Figure 1 and larger aggregates could be easily found in the sample. The higher degree of agglomeration can be attributed to the higher concentration of NaCl in the reaction mixture.

We can use the DLVO theory to explain the formation of dimers and the dependence of yield on the concentration of NaCl. DLVO, a theory proposed by four renowned scientists Derjaguin, Landau, Verwey, and Overbeek during the 1940s, provides basic framework for colloidal interactions and colloidal stability (the theory became known by the initial letters of their names: DLVO). In the DLVO theory, colloidal stability is determined by a balance between the short-range double-layer repulsion and long-range van der Waals attraction.<sup>24</sup> As two particles approach each other, a repulsive barrier appears due to the electrostatic repulsion between the double layers. When the repulsive barrier is greater than  $10k_{\text{B}}T$ , where  $k_{\text{B}}$  is the Boltzmann constant and  $T$  is the temperature, the collisions derived from Brownian motion will be unable to overcome the barrier and thus induce agglomeration. However, when the repulsive barrier is reduced to the scale below  $10k_{\text{B}}T$ , it is highly possible that dimerization, as well as higher degrees of aggregation, will occur in the suspension as a result of the constant collisions between colloidal particles derived from Brownian motion. In the diffusive double layer, the repulsive electrostatic potential  $V_{\text{R}}$  can be expressed by the following equation:<sup>24</sup>

$$V_{\text{R}}(h) \propto k^{-1}e^{-kh} \quad (1)$$

where  $h$  is the separation distance between two particles, and  $k$  is the inverse Debye length. In general,  $k$  is given by

$$k = \left( F^2 \sum_i c_i z_i^2 / \epsilon_0 \epsilon R T \right)^{1/2} \quad (2)$$

where  $F$  is the Faraday constant,  $\epsilon_0$  is the permittivity of vacuum,  $\epsilon$  is the dielectric constant of the dispersion medium,  $R$  is the ideal gas constant, and  $c_i$  and  $z_i$  are the concentration and valence of the counterion of type  $i$ . On the basis of eq 2, the easiest way to control  $k$  is to vary the concentration and nature of the electrolytes or ionic species. A decrease in the electrolyte concentration will result in relatively good stability for the colloidal system, while an increase in the electrolyte concentration will yield an unstable system, inducing dimerization and higher degrees of aggregation for the colloidal particles. In order to optimize the yield of dimers, one has to control the concentration of NaCl in the medium region, not too low or too high.

We also performed correlated SERS/SEM measurements on the dimers of nanospheres.<sup>25</sup> In a typical procedure, the sample was prepared by drop-casting an ethanol suspension of the dimers on a Si substrate that had been patterned with registration marks and letting it dry under ambient conditions. Once the sample had dried, it was rinsed with copious amounts of ethanol, immersed in a 5 mM solution of 4-methyl-benzenethiol (4-MBT, Aldrich) in ethanol for 3 h, taken out, washed with copious amounts of ethanol, and finally dried under a stream of nitrogen. All samples were used immediately for SERS measurement after preparation. The SERS spectra were recorded using a Renishaw inVia confocal Raman spectrometer coupled to a Leica microscope with 50 $\times$  objective in backscattering geometry. The 785 nm output from a diode laser was used as the excitation source, together with a holographic notch filter. The backscattered Raman signals were collected on a thermoelectrically cooled ( $-60$   $^{\circ}\text{C}$ ) charge-coupled device. The scattering spectra were recorded in the range of 800–2000  $\text{cm}^{-1}$ , in one acquisition, 30 s accumulations, and 1.5 mW at the sample. All data were baseline corrected by subtracting the background signals from Si.

Figure 4 shows SERS spectra taken from the sample that had been functionalized with 4-MBT. Owing to the relatively small size ( $\sim 30$  nm in diameter) of the silver nanospheres, we expect that probe molecules outside the hot spot region will not contribute to the detected SERS signals.<sup>26</sup> Hence, our dimers provide an ideal model system for investigating the enhancement factor and polarization effect of an individual hot spot. The top trace in Figure 4A shows the SERS spectrum taken from a single dimer with the laser polarization parallel to the longitudinal axis. The two characteristic peaks for 4-MBT at 1079 and 1594  $\text{cm}^{-1}$  were clearly resolved, albeit at low intensity. The peak at 1079  $\text{cm}^{-1}$  is due to a combination of the phenyl ring-breathing mode, CH in-plane bending, and CS stretching, while the peak at 1594  $\text{cm}^{-1}$  can be assigned to phenyl stretching motion (8a vibrational mode).<sup>27,28</sup> The low intensity reflects the small number of molecules trapped in the hot spot region and the relatively smaller Raman cross-section for the 4-MBT molecules as compared to organic dyes usually employed in single-molecule SERS studies.<sup>4-6</sup> Figure 4A also gives the SERS spectra recorded from two silver nanospheres separated by  $\sim 600$  nm (middle trace) and a single silver nanosphere (bottom trace). In these two cases, there was no hot spot involved. In the case of two silver nanospheres separated by 600 nm, both of them were within the laser focal volume ( $\sim 10$   $\mu\text{m}$  in diameter), and the total number of probed 4-MBT molecules should be similar to the case of a dimer. The absence of detectable SERS signals confirm that only 4-MBT molecules trapped in the hot spot region are responsible for the SERS peaks at 1079 and 1594  $\text{cm}^{-1}$ .

We employed the peak at 1079  $\text{cm}^{-1}$  to estimate the enhancement factor (EF) of the hot spot through the following equation:

$$EF = (I_{\text{sers}} \times N_{\text{bulk}}) / (I_{\text{bulk}} \times N_{\text{trap}}) \quad (3)$$

where  $I_{\text{sers}}$  and  $I_{\text{bulk}}$  are the intensities of the same band for the SERS and bulk spectra,  $N_{\text{bulk}}$  is the number of bulk molecules probed for a bulk sample, and  $N_{\text{trap}}$  is the number of molecules probed in the SERS spectrum. The areas of the 1079  $\text{cm}^{-1}$  band were used for the intensities  $I_{\text{sers}}$  and  $I_{\text{bulk}}$ . We chose this band because it was the strongest band in the spectra.  $N_{\text{bulk}}$  was determined based on the Raman spectrum of a 0.1 M 4-MBT solution in 12 M  $\text{NaOH}_{(\text{aq})}$  and the focal volume of our Raman system (1.48 pL). When determining the number of trapped molecules ( $N_{\text{trap}}$ ) in the hot spot region, we assume that the 4-MBT molecules will be absorbed as a monolayer with a 0.19  $\text{nm}^2$  molecular footprint onto a spherical cap having  $h = r/6.6$  located on each silver nanosphere of the dimer (i.e., the interparticle region), as shown in Figure 4B. This approximation was based on the TEM images shown in Figure 1C,D, and yielded  $N_{\text{trap}} = 2510$ . This number represents a theoretical maximum number of molecules and is surely an overestimate, thus the EF reported here is likely an underestimate rather than an overestimate of the actual EF value. According to this approach, the EF of the hot spot was calculated to be  $1.9 \times 10^7$ . Alternatively, if we assume that the hot spot region is enclosed by two hexagonal (111) faces (see the inset in Figure 1C),  $N_{\text{trap}} = 1904$  and the EF became  $2.5 \times 10^7$ , which is also close to  $1.9 \times 10^7$ . It is important to note that 4-MBT does not exhibit any absorption bands around 785 nm, which excludes the possibility of any resonance Raman effects for the excitation laser employed in our study. Further enhancement of the SERS effect can be achieved by employing probe molecules with resonance effects and/or by optimizing the laser wavelength employed in the measurements.

Figure 5 illustrates the dependence of the SERS signals on the laser polarization for the silver nanosphere dimer. It can be observed that the 4-MBT peaks were maximized when the laser was polarized parallel to the longitudinal axis of the dimer. The 4-MBT signals were gradually reduced when the laser was rotated by 22.5 and 45° away from the longitudinal axis. At 45°, the area of the peak at 1079  $\text{cm}^{-1}$  was reduced by a factor of  $\sim 3$ . Finally, the 4-MBT peaks disappeared when the polarization was off from the longitudinal axis by angles larger than 45° (e.g., 77 and 90°).



In summary, we have prepared dimers of single-crystal silver nanospheres in reasonably high yields through a facile, one-step method based on the polyol reduction. The amount of NaCl added to the reaction solution played a critical role in determining the yield of the dimers. By controlling the concentration of NaCl, we were able to optimize the conditions for both oxidative etching and dimerization. The dimers were SERS active and could serve as an ideal system for investigating the hot spot phenomenon. With 4-MBT as a probe molecule, the enhancement factor for the hot spot region of a silver nanosphere dimer was estimated to be  $1.9 \times 10^7$ . The SERS signals taken from the hot spot were polarization dependent; they were maximized when the laser was polarized parallel to the longitudinal axis and vanished when the polarization was in the orthogonal direction. We believe that these well-defined dimers hold great promise for ultrasensitive detection and even single-molecule detection by SERS and are expected to find a range of applications in fields such as life sciences, environmental science, and photonics.

## Acknowledgment

This work was supported in part by research grants from the NSF (DMR, 0451788 and 0804088) and a Director's Pioneer Award from the NIH(5DP1OD000798). P.H.C.C. was supported in part by the Fulbright Program and the Brazilian Ministry of Education (CAPES).

## References

1. Stiles PL, Dieringer JA, Shah NL, Van Duyne RP. *Annu. Rev. Anal. Chem* 2008;1:601.
2. Banholzer MJ, Millstone JE, Mirkin CA. *Chem. Soc. Rev* 2008;37:885. [PubMed: 18443674]
3. Kneipp K, Kneipp H, Itzkan I, Dasari RR, Feld MS. *Chem. Rev* 1999;99:2957. [PubMed: 11749507]
4. Nie S, Emory SR. *Science* 1997;275:1102. [PubMed: 9027306]
5. Kneipp K, Wang Y, Kneipp H, Perelman LT, Itzkan I, Dasari RR, Feld MS. *Phys. Rev. Lett* 1997;78:1667.
6. Camden JP, Dieringer JA, Wang Y, Masiello DJ, Marks LD, Schatz GC, Van Duyne RP. *J. Am. Chem. Soc* 2008;130:12616. [PubMed: 18761451]
7. Glotzer SC, Solomon MJ. *Nat. Mater* 2007;6:557. [PubMed: 17667968]
8. Whitesides GM, Grzybowski BA. *Science* 2002;295:2418. [PubMed: 11923529]
9. Klajn R, Bishop KJM, Fialkowski M, Paszewski M, Campbell CJ, Gray TP, Grzybowski BA. *Science* 2007;316:261. [PubMed: 17431176]
10. Rycenga M, McLellan JM, Xia Y. *Adv. Mater* 2008;20:2416.
11. Alivisatos AP, Johnsson KP, Peng XG, Wilson TE, Loweth CJ, Bruchez MP, Schultz PG. *Nature* 1996;382:609. [PubMed: 8757130]
12. Loweth CJ, Caldwell WB, Peng XG, Alivisatos AP, Schultz PG. *Angew. Chem., Int. Ed* 1999;38:1808.
13. Mirkin CA, Letsinger RL, Mucic RC, Storhoff JJ. *Nature* 1996;382:607. [PubMed: 8757129]
14. Park SY, Lytton-Jean AKR, Lee B, Weigand S, Schatz GC, Mirkin CA. *Nature* 2008;451:553. [PubMed: 18235497]
15. Novak JP, Feldheim DL. *J. Am. Chem. Soc* 2000;122:3979.
16. Sardar R, Heap TB, Shumaker-Parry JS. *J. Am. Chem. Soc* 2007;129:5356. [PubMed: 17425320]
17. Wang X, Li G, Chen T, Yang M, Zhang Z, Wu T, Chen H. *Nano Lett* 2008;8:2643. [PubMed: 18672944]
18. Moskovits M. *J. Raman. Spectrosc* 2005;36:485.
19. Wiley B, Sun Y, Xia Y. *Acc. Chem. Res* 2007;40:1067. [PubMed: 17616165]
20. Wiley B, Herricks T, Sun Y, Xia Y. *Nano Lett* 2004;4:1733.
21. Kim MH, Lu X, Wiley B, Lee EP, Xia Y. *J. Phys. Chem. C* 2008;112:7872.
22. Sun Y, Mayers B, Herricks T, Xia Y. *Nano Lett* 2003;3:955.
23. Hao E, Schatz GC. *J. Chem. Phys* 2004;120:357. [PubMed: 15267296]

24. Evans, DF.; Wennerström, H. *The Colloidal Domain: Where Physics, Chemistry, Biology, and Technology Meet*. 2nd ed.. Wiley; New York: 1999. Chapter 8
25. McLellan JM, Li Z-Y, Siekkinen AR, Xia Y. *Nano Lett* 2007;7:1013. [PubMed: 17375965]
26. Le Ru EC, Etchegoin PG, Meyer M. *J. Chem. Phys* 2006;125:204701. [PubMed: 17144717]
27. Sauer G, Brehm G, Scheneider S. *J. Raman Spectrosc* 2004;35:568.
28. Osawa M, Matsuda N, Yoshii K, Uchida I. *J. Phys. Chem* 1994;98:12702.

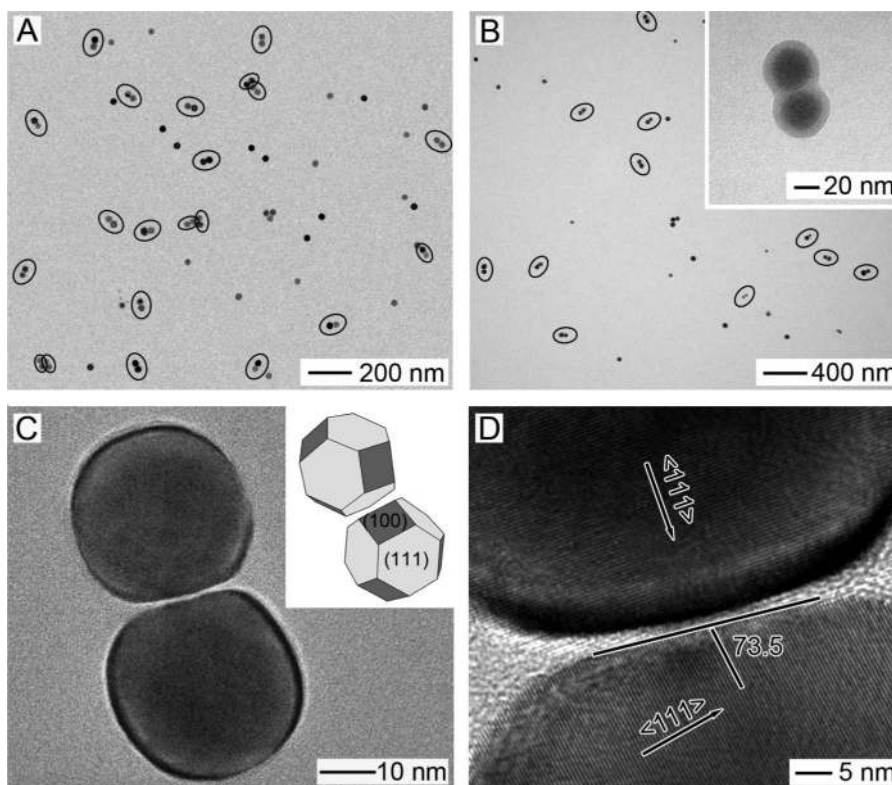


**Figure 1.** (A,C) TEM images of silver nanosphere dimers at two different magnifications. (B) TEM image of the silver nanosphere dimers after their surface had been coated with silica. The dimers are highlighted by black ellipses. The inset in (B) shows a magnified TEM image of the sample. The inset in (C) gives a schematic illustration of the silver nanospheres in the dimer. (D) HRTEM image of the gap in a silver nanosphere dimer. Experimental condition: temperature, 145 °C; the amount of NaCl/EG solution (10 mM) added, 90  $\mu$ L; and reaction time,  $\sim$ 20.5 h.



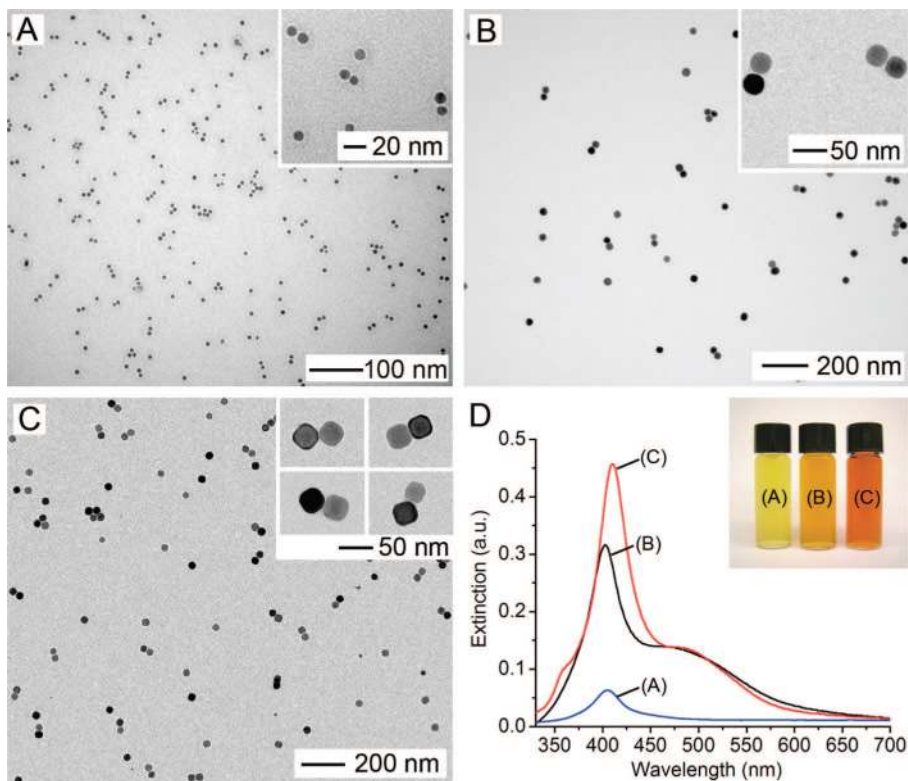


**Figure 2.** TEM images of samples obtained at three different stages of the reaction. The samples were taken when the color of the reaction mixture was (A) light yellow (~19 h), (B) bright yellow with a slight orange tint (~20.5 h), and (C) and dark orange yellow with a slight red-brown tint (~21 h). The insets show magnified TEM images of the samples. The inset in (C) shows dimers of cubic silver nanoparticles that were formed by interacting with different types of facets. (D) UV-vis extinction spectra of the samples taken at different reaction states. Experimental condition: temperature, 145 °C; and the amount of NaCl/EG solution (10 mM) added, 90  $\mu$ L.

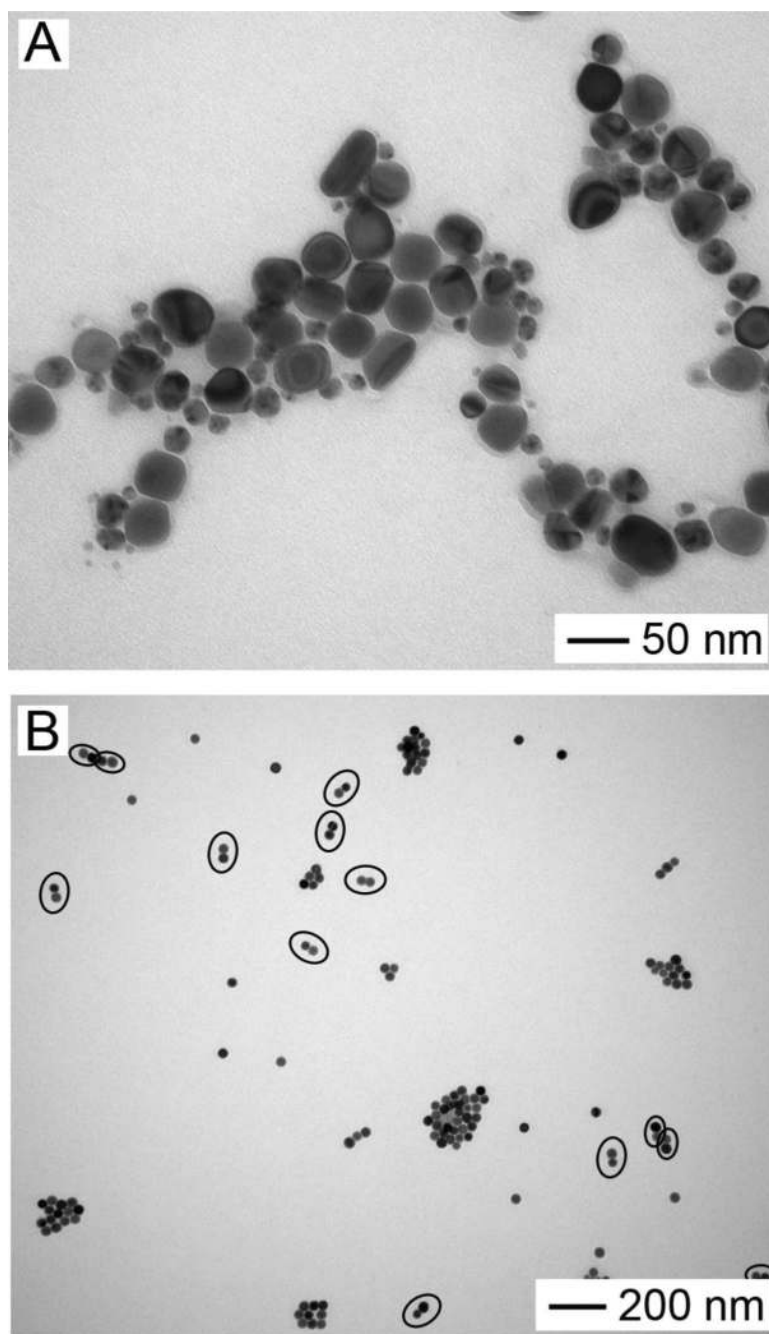


**Figure 3.** TEM images of samples prepared with the addition of different amounts of NaCl/EG solution (10 mM): (A) 66  $\mu\text{L}$  and (B) 114  $\mu\text{L}$ . The reaction temperature was 145  $^{\circ}\text{C}$ . The dimers are highlighted by black ellipses in (B).

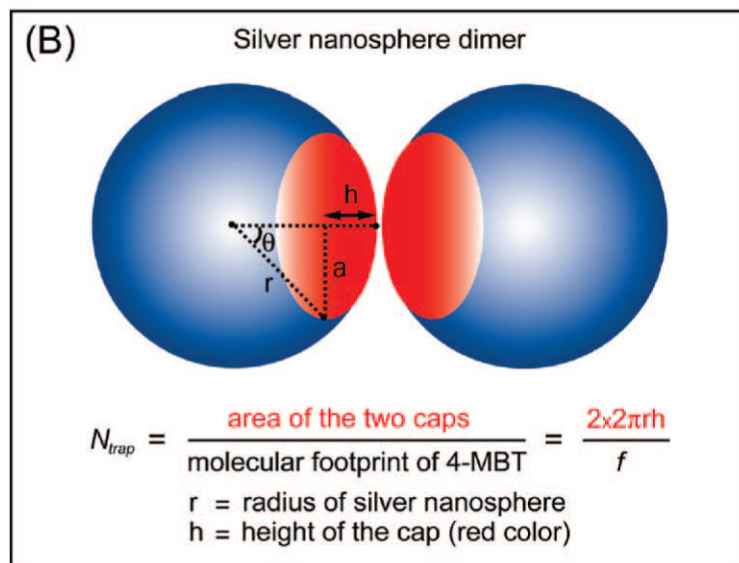
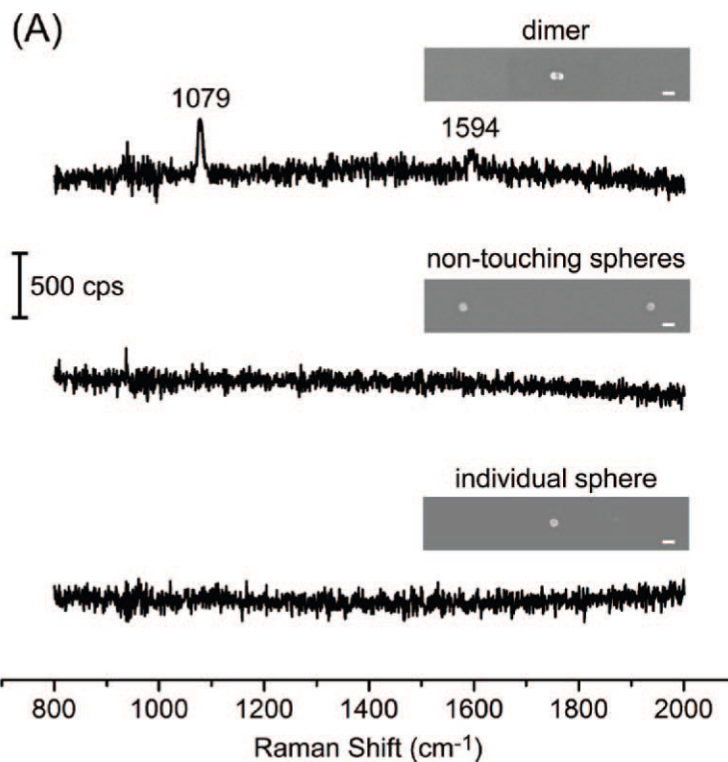


**Figure 4.**

(A) SERS spectra taken from (top) a dimer of silver nanospheres, (middle) two silver nanospheres separated by  $\sim 600$  nm, and (bottom) a single silver nanosphere. The scale bars in the insets correspond to 50 nm. (B) A schematic showing our approach to estimate the number of probe molecules trapped in the hot spot ( $N_{\text{trap}}$ ) of a dimer. The hot spot region is assumed to comprise a cap on the surface of each nanosphere in the interparticle region of the dimer (red color).  $N_{\text{trap}}$  is obtained by calculating the total surface area of the hot spot region (surface area of the two caps) and dividing it by the molecular footprint of a 4-MBT molecule. In our calculations,  $h = r/6.6$  (where  $h$  is the height of the cap and  $r$  is the radius of the nanosphere).

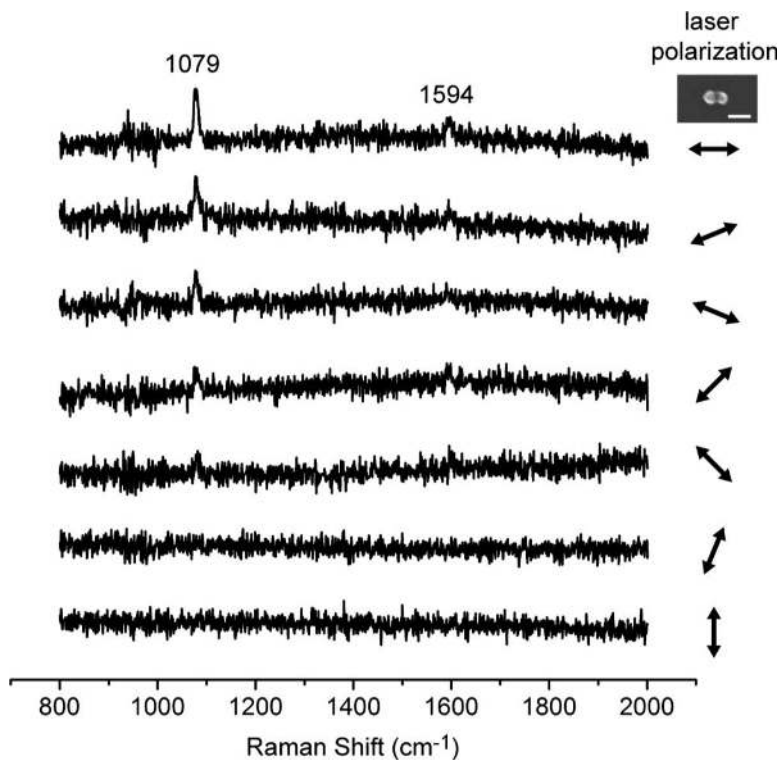


**Figure 5.** SERS spectra taken from a dimer of silver nanospheres (same as the one shown in Figure 4A) under different orientations relative to laser polarization. The 4-MBT peaks were maximized when the laser polarization was parallel to the longitudinal axis of the dimer. All spectra were taken with 785 nm excitation laser, 30 s accumulation, 1.5 mW at the sample. The scale bar in the inset corresponds to 50 nm.